Audio Engineering Society

Convention Paper 9599

Presented at the 141st Convention
2016 September 29 – October 2, Los Angeles, CA, USA



# Fully Coupled Time-Domain Simulations of Loudspeaker Transducer Motors

Andri Bezzola[1] and Pascal Brunet[1]

[1] *Samsung Research America, DMS Audio, Valencia CA 91355*

Correspondence should be addressed to Andri Bezzola (andri.b@samsung.com)

**ABSTRACT**

We present a novel time-dependent simulation method to calculate the response of a loudspeaker motor. The model allows for the simulation of complex signals and predicts the large-signal behavior including motor nonlinearities using only the motor geometry and material parameters without the need to measure physical samples. The transient large-signal simulation is made possible by the implementation of a moving-mesh algorithm for the displacement of the voice coil. Two motor geometries are simulated with different input signals, ranging from simple sine to complex random signals. The method provides previously unavailable insight into effects of flux modulation. The results are validated against a lumped parameter model and experimental measurements. The presented method can be used to compare different motor geometries before the prototyping stage, which is a useful tool for loudspeaker transducer engineers.

## 1 Introduction

Numerical models of electromagnetic loudspeaker motors based on methods such as the Finite Element (FE) method, have been used to reduce the costly iterative process of prototype manufacturing and testing [1, 2]. These methods have been particularly successful at predicting the linear small-signal parameters, such as the *Bl* value or inductance at rest position of the voice coil. Modern FE software readily allows for the coupling of electrical, magnetic, structural, and acoustic components of a loudspeaker system [3]. Such simulations are typically carried out in the frequency domain and are as such - by definition - linear.

Some techniques, such as the blocked-coil method [4, 5], can be applied to the frequency-domain simulations to infer certain nonlinear effects [6, 7] and predict the dominant causes of distortion [8]. However, these methods do not take into account the nonlinear dynamics of the loudspeaker as it is pushed and pulled through the magnetic field, creating a back EMF and exhibiting forces due to reluctance. An additional nonlinear lumped-parameter (LP) model is typically needed to determine the total distortion caused by the loudspeaker motor or to auralize the simulated signal and fully predict total distortion based on FE parameter predictions. An example of such a nonlinear LP model can be found in [9].

This paper proposes a method that does not require the combination of a LP model in conjunction with

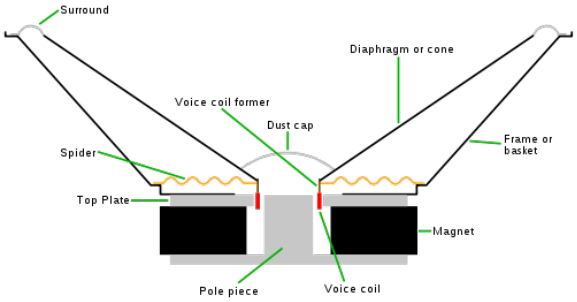


**Fig. 1:** Loudspeaker mechanism.

the FE model to predict the nonlinear behavior of the loudspeaker motor for a certain sound or music signal. A time-dependent electromagnetic FE model, resolving the electric and magnetic fields in and around the motor structure, is fully coupled to an ordinary differential equation that describes the dynamic motion of the voice coil. The result is a direct extraction of the voice coil position, velocity, acceleration and current for a given input signal. Direct estimation of distortion due to motor nonlinearities can be calculated in a single step.

In order to simulate large enough displacements of the voice coil we introduce a moving-mesh technique that prevents excessive mesh deformation due to large voice coil movement. We use the proposed model to simulate the response of the driver to two different input signals, a simple sine and a more complex pseudomusic signal. Comparing the acceleration of the voice coil with the input signal, it is possible to quantify the distortion caused by the motor elements. We analyze harmonic distortion as well as total distortion. Finally, we compare results with measurements of a physical transducer and an established LP model that uses the small and large signal parameters from the measured transducer.

## 2 Methods

We briefly discuss the LP model first, then explain in detail how we set up the FE model, and finally touch on the experimental setup for measurement

### 2.1 LP Motor Model

The LP model is the traditional model used to describe electrodynamic loudspeaker as the one shown in Figure 1. Using the following definitions:

- $u$ : Voltage at the voice coil terminal
- $i$ : Current in the voice coil
- $x$ : Voice coil excursion
- $v$ : Voice coil velocity
- $Bl(x)$ : Force factor as function of $x$
- $K_{ms}(x)$ : Suspension stiffness as function of $x$
- $L_e(x)$ : Voice coil inductance as function of $x$
- $M_{ms}$ : Moving mass
- $R_{ms}$ : Mechanical resistance
- $R_e$ : Electrical resistance

the dynamics of the loudspeaker is described by the two following coupled ordinary differential equations (ODE) [9]:

$$u = R_e\, i + Bl(x)v + \frac{d(L_e(x)i)}{dt} \tag{1}$$

$$Bl(x)i = M_{ms}\frac{dv}{dt} + R_{ms}\, v + K_{ms}(x)x - \frac{1}{2}\frac{dL_e(x)}{dx}i^2 \tag{2}$$

where the dependence of $L_e$ vs current is neglected. The system is nonlinear due to the dependence of $Bl, K_{ms}, L_e$ on the position $x$ (see Figure 5).

Reorganizing equations (1) and (2) to a state-space model with state vector $X = [x, v, i]^T$, we get :

$$\begin{aligned}
\frac{dx}{dt} &= v \\
\frac{dv}{dt} &= -\frac{1}{M_{ms}}(K_{ms}(x)x - R_{ms}\, v + Bl(x)i + \frac{1}{2}\frac{dL_e(x)}{dx}i^2) \\
\frac{di}{dt} &= \frac{1}{L_e(x)}(-Bl(x)\, v - R_e\, i - \frac{dL_e(x)}{dx}\, v\, i + u).
\end{aligned} \tag{3}$$

Equations (3) can be summarized in the following nonlinear state-space equation:

$$\dot{X} = f(X) + g(X)u$$

where $f, g$ are smooth vector-fields $\mathbb{R}^3 \to \mathbb{R}^3$. For numerical time evolution, we use the forward Euler approximation:

$$\dot{X}_k \approx \frac{(X_{k+1} - X_k)}{T_s}$$

with $T_s$ is the sampling period and $k$ is the sample index.

We obtain our parameters $Bl(x)$, $K_{ms}(x)$, $L_e(x)$, $M_{ms}$, $R_{ms}$, and $R_e$ from physical measurements using a Klippel LSI scanner.

### 2.2 The FE Motor Model

The objective of this work is the quantification of the distortion in electromagnetic elements of the loudspeaker on the input signal by a single simulation step. We assume explicit knowledge of the structural dynamic behavior of the moving parts; that is we adopt the model for the mechanical parts from the LP model.

What remains to be calculated via FE modeling are the electromagnetic components of a loudspeaker driver. We are simulating the spatial and temporal behavior of the currents and magnetic potential field via a time-dependent FE model. In particular, we are solving Ampère's law for materials with different electromagnetic properties. The most important are outlined in the following paragraphs.

#### 2.2.1 Materials

We assume that the permanent magnets in the loudspeaker operate in the linear $BH$ domain with remanent flux density $B_{rM}$ and relative permeability $\mu_{rM}$. Values for specific examples are given in Table 1. Additionally, we consider the case where the magnet material is conductive. This is important to properly calculate the induced currents [10].

A typical loudspeaker motor operates in the nonlinear point of the steel magnetic saturation curve. Some parts of the steel are close to saturation, while others are far from saturation. It is therefore necessary to consider the nonlinear $BH$ behavior of the steel used in the motor. Without current flowing through the voice coil, the permanent magnet generates a static $H$-field and $B$-field in the steel parts and in the voice coil gap. This static $H$-field gets modulated by the AC current that flows through the moving voice coil, which in turn also modulates the $B$-field in the steel parts and the voice coil gap in a nonlinear way.

Due to the strong nonlinearity of the $BH$ relationship in steel it can be difficult to achieve numerical convergence of the solver when very complex signals are applied. For the test cases, we linearized the permeability of each point in space around the static $H$-field that is generated by the permanent magnets. As can be seen in Figure 2, the effective linearized permeability in steel is close to zero for the saturated areas. The areas in the steel parts with least saturation are closer to the linear steel value of $\mu_r = 2500$. Essentially, the

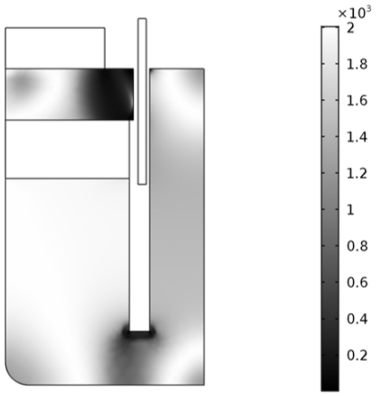


**Fig. 2:** The static relative permeability distribution $\mu_r(\vec{r})$ in a cross section of motor assembly. Dark areas are close to saturation. Unsaturated areas are white.

linearized $BH$-relationship at each point $\vec{r} = (r,z)$ in space becomes

$$B(\vec{r}) = \mu_0 \mu_r(\vec{r}) H(\vec{r}), \tag{4}$$

with $\mu_0$ the permeability of vacuum. Throughout the time-dependent simulation $\mu_r(\vec{r})$ is kept time invariant.

Some loudspeaker motors use conductive shorting rings to reduce the distortion due to inductance [11] and reduction in the flux modulation [12]. While the shorting ring material is modeled linearly, they still affect the signal nonlinearly, because the effect is dependent on position, velocity and current in the voice coil.

The voice coil is modeled as a multi-turn voice coil. The multi-turn coil feature in COMSOL [3] implements a homogenized model of a coil consisting of numerous tightly-wound conducting wires. The computation of the voltage and current of the coil takes into account parameters such as the number of turns and wire diameter. This feature is useful to model a coil containing a large number of wires without the need to model each wire individually.

The voice coil and the induced currents in the steel parts form a multi-turn to single-turn transformer. This means that the induced currents in the steel parts also induce a small current back into the voice coil. This effect is assumed to be minimal and is not considered in this work. However, Lorentz type effects are considered in this work; the voice coil moves in a $B$-field

which creates a back-EMF that opposes the coil's motion. We consider this effect by applying an effective voltage at the voice coil terminals that is dependent on the instantaneous $B$-field at the position of the voice coil and on the velocity of the voice coil:

$$V_{VC}(t) = V_{in}(t) - Bl(x(t))\dot{x}(t) \tag{5}$$

where $V_{VC}$ is the resulting potential drop over the voice coil wire, $V_{in}(t)$ is the applied voltage signal, $Bl(x(t))$ is the instantaneously felt force factor and $\dot{x}(t)$ is the voice coil velocity. The electromagnetic force on the voice coil can be calculated as:

$$F_{EM}(t) := Bl(x(t))\, i_{VC}(t) \tag{6}$$

$$= \overline{B_r}(x(t))\, 2\pi r_{VC}\, N_0\, i_{VC}(t)\,. \tag{7}$$

$i_{VC}(t)$ is current in the voice coil, $2\pi r_{VC} N_0$ is the length $l$ of the voice coil wire, and $\overline{B_r}(x(t))$ is the radial component of the $B$-field averaged over the cross section area of the voice coil at position $x(t)$.

#### 2.2.2 FE Model Setup

The voice coil is coupled to an ODE that conserves momentum of the voice coil, former, diaphragm, and suspension elements. The moving parts have a total mass of $M_{ms}$ and a total damping parameter $R_{ms}$. The suspension elements act with a nonlinear restorative force $K_{ms}$ that is dependent on the voice coil position $x(t)$. The concept of coupling the electromagnetic FE model to an ODE is shown in Figure 3.

While it is possible to model the structural dynamics of the moving parts in a FE fashion, it would require substantially more computation power. Additionally, several material parameters including damping values and modulus of elasticity for the moving parts can be nonlinear and dependent on position and velocity. We therefore omit the costly FE calculation of the moving parts, and focus on the direct simulation of the distortion caused by the electromagnetic motor elements.

In order to properly study distortion on a sound signal caused by the electromagnetic elements of a loudspeaker driver, it is necessary to use a framework that allows for large displacement of the voice coil. We implement a moving-mesh technique in our FE model that lets the voice coil undergo a one-dimensional rigid body translation $x(t)$. The rest position of the voice coil is set such that $x = 0$ when no current is applied.

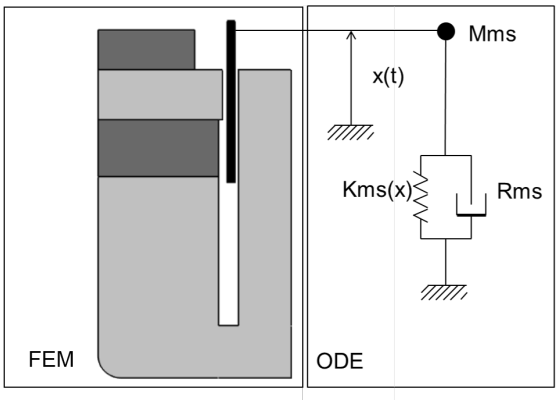


**Fig. 3:** The electromagnetic components of the loudspeaker motor are coupled at the voice coil to the dynamic mechanical parts via a momentum conservation ODE for a spring-damper-mass system.

While the voice coil mesh undergoes translation, it does not get deformed in the sense that it is stretched or warped. But the area around the voice coil needs to let the FE mesh deform elastically, such that it can bridge the rigidly moving voice coil and the remaining static mesh. In COMSOL this can be accomplished by the "Deformed Mesh" utility.

The FE models are solved in two steps. In step one we solve a static solution with fully nonlinear $BH$ behavior and no applied voltage to get the locally varying linearization point $\mu_r(\vec{r})$.This step is generally solved in a matter of several seconds on a modern desktop computer (2.5 GHz) with enough RAM memory for the problem at hand.

The time-dependent part of the solving process uses the linearized model for the $BH$ behavior of steel from Equation (4). The solution is calculated with an adaptive time step backward differentiation formula (BDF) [13]. Care was taken to force the solver's output at the desired sampling frequency. Typical solver times observed were around 12 hours for a signal of 1 s on a 2.5 GHz desktop computer with 4 cores and 64 GB of RAM. The solver time varies with the complexity of input signal, where broadband signals take longest to complete.

### 2.3 Driver Geometries and Parameters

Figure 4 shows the geometries used for the simulations and measurements presented in Section 3. The geome-

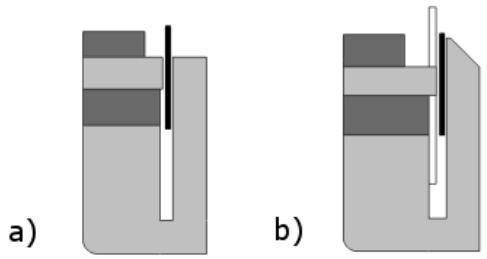


**Fig. 4:** Cross sections of the geometries used for the simple motor without shorting rings (a) and improved motor with raised pole and shorting rings (b).

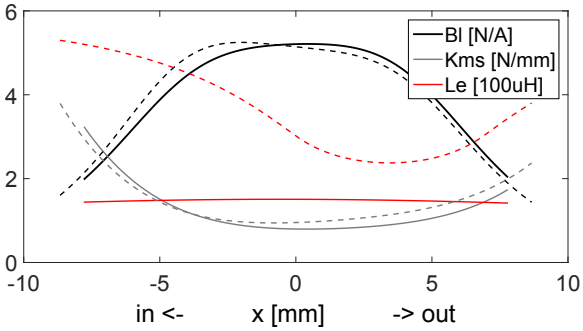


**Fig. 5:** Large signal parameters for the simple motor (dashed) and for the improved motor (solid). $L_e(x)$ and $Bl(x)$ are much more symmetric for the improved geometry.

tries are taken from a 5-inch woofer that has been used for development at the Samsung Audio Lab. The simpler model in Figure 4a) is driven by two neodymium magnets that have been magnetized to $B_{rM} = 1.3$ T. The second magnet acts as a bucking magnet to improve $B$-field symmetry. It does not have any type of shorting elements to improve inductance or flux modulation. The improved model in Figure 4b) uses two copper shorting rings that reduce the inductance and flux modulation. It also has a modified pole geometry further increasing symmetry of the $B$-field.

The parameters used for the simple motor and the improved motor geometry shown in Figure 4 are given in Table 1 and the non-linear $Bl(x)$ and $K_{ms}(x)$ are plotted in Figure 5. For the steel parts and shorting rings we used the standard values in COMSOL for soft magnetic steel 1008 and copper respectively. The voice coil is assumed to be made of copper clad aluminum wire.

### 2.4 Measurements

The improved woofer with shorting rings was measured in free air to validate our models. The following quantities have been acquired over time to fully capture the dynamics of the driver:

- $u$ : Voltage at the voice coil terminal
- $i$ : Current in the voice coil with a shunt resistor of 0.1 Ohms in the return path of the amplifier.
- $x$ : Cone excursion with a LASER vibrometer
- $p$ : Sound pressure with a microphone in the near field

Two excitation signals have been used. First, a sine wave at 50 Hz, below resonance frequency of driver, to ensure a maximum displacement. Second, a pseudo-music signal, which is a simulated signal whose mean power spectral density closely resembles the average of mean power spectral densities of a wide range of program material. Its amplitude distribution is Gaussian, which closely resembles the average amplitude distribution of music and speech [14]. The level of excitation signals has been chosen to reach a maximum of 5 mm excursion.

## 3 Results

### 3.1 Simple Sine Stimulus

The first results are shown for simulations of a sine wave of 50 Hz. Simulations were run at a sampling frequency of $F_s = 12$ kHz for the duration of 1 s. As the FE simulations solve for the electric field, they can directly be used to calculate the $Bl(x)$ curve. The $B$-field is modulated during the time-dependent simulation by the current in the moving voice coil. This means that the $Bl$ values can vary over time for any given position $x$.

We can calculate the instantaneous $Bl(x(t))$ value from Equation (7) by realizing that $2\pi r_{VC} N_0$ is the total length $l$ of the voice coil wire. In order to visualize the $Bl$ values we can draw a phase plot of $Bl(x(t))$ against the voice coil position $x(t)$. We can also evaluate Equation (4) for the static solution to get a single $Bl(x)$ curve. In Figures 6a) and 6b) we show the phase plot and the static solution as computed in the simulation and compare it with the measured $Bl(x)$ curve obtained by the Klippel LSI measurement.

**Table 1:** Parameters used for the simulations of the two motor structures used in the examples.

| Parameter | Simple Motor | Improved Motor | Description |
|---|---|---|---|
| $B_r$ | 1.3 T | 1.3 T | Remanent flux density of permanent magnet |
| $\mu_{rM}$ | 1.05 | 1.05 | Relative permeability of permanent magnet |
| $\sigma_{neo}$ | $6.666 \cdot 10^5$ S/m | $6.666 \cdot 10^5$ S/m | Conductivity of permanent magnet |
| $R_{DC}$ | 3.88 Ω | 3.71 Ω | DC resistance of voice coil |
| $N_0$ | 83.6 | 83.6 | Number of coil windings |
| $d_{coil}$ | 0.3 mm | 0.3 mm | Diameter of voice coil wire |
| $M_{ms}$ | 9.28 g | 8.85 g | Total mass of moving elements including air load |
| $R_{ms}$ | 0.482 kg/s | 0.400 kg/s | Total losses in moving elements |

When comparing the *Bl* curves in Figure 6, three major results stand out: First, the measured and simulated $Bl(x)$ curves of the improved driver differ by a substantial amount. Additional work will be needed to fully explain this discrepancy. Some potential explanations are given in Section 4. Second, the simple motor structure shows some asymmetry around $x$=0. The improved motor structure is much more symmetric. Third, the spread between individual passes of $Bl(x(t))$ is about 0.01 N/A for the simple motor structure and 0.004N/A for the improved motor structure. This indicates that the latter exhibits less flux modulation from the moving voice coil.

We can plot the voice coil position, velocity, acceleration, and current as a function of time, and compare FE simulation, LP simulation, and experimental results. These values are directly accessible from the simulations and do not require any kind of post-processing. Figure 7a) shows the position of the voice coil for the three different cases. The position predicted by the LP model and the measured position are indistinguishable. The position predicted by the FE model appears to lack about a 0.2 mm excursion at the extrema. The relative root means square error (rRMSE) is 4.63 % for the FE model and 0.66 % for the LP model when compared to the measurement.

Similarly, one can plot velocity and acceleration of the voice coil. For brevity, we omit the plot of the velocity for this example, but the acceleration is shown in Figure 7b). It is notable that even though the extrema of the acceleration plot are slightly underestimated, the FE model is still tracking the distorted shape of the measurement and the LP model. The rRMSE values are 7.60 % for the FE model and 0.60 % for the LP model respectively.

Lastly we show the results for the current in the voice coil for the FE and LP models and the measurement. The current curves are shown in Figure 7c). Interestingly, the current simulated in the FE model tracks the measured current accurately until about 0.02 s, at which point the amplitude and shape both deviate from the measured values. The rRMSE values are 15.9 % for the FE model and 0.7 % for the LP model. The authors do not have an explanation for this discrepancy at this point, but it will be subject of further investigation.

The result for the voice coil acceleration was put through a Discrete Fourier Transform (DFT) to analyze the frequency content of the resulting signal. A simulated signal length of 1 s with a sampling frequency $F_s$ of 12 kHz, we obtain a result up to the Nyquist frequency of 6 kHz with spectral spacing of 5 Hz. The results and comparison between FE and LP model and the measured response is shown in Figure 8. Again, the difference between LP model and measurement was undetectable. The result for the FE model reproduces the harmonic distortion peaks astonishingly well all the way up to the 6th harmonic. This result is surprising and encouraging, confirming that the presented methodology can indeed be used for distortion analysis using time-domain signals. The FE model does produce a higher level of noise than the LP model and measurement, but the noise level is still about 70 dB below the harmonic peaks.

### 3.2 Pseudomusic Stimulus

The second set of results presented are simulations and measurements of a pseudomusic signal in the improved driver geometry. As discussed in Section 2, pseudomusic has a spectral density that is representing a wide range of program material. In order to keep the simulation time within reasonable bounds we applied a 6 kHz

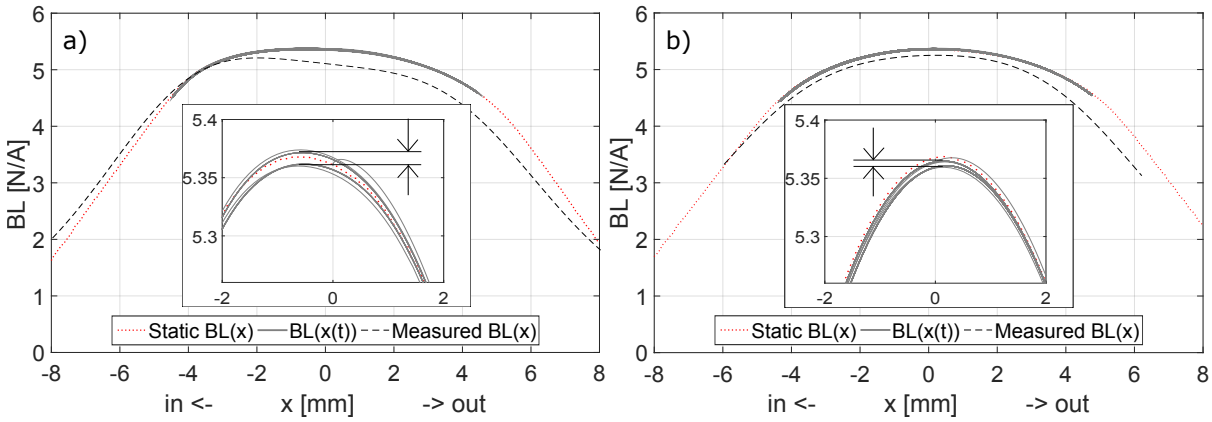


**Fig. 6:** Simulated and measured $Bl(x)$ curves of the simple motor (a) and the improved motor (b). The insets show the amount of flux modulation around the rest position $x = 0$. At the arrows, the spread between the curves is 0.01 N/A for the simple geometry and 0.004 N/A for the improved geometry.

low-pass filter to the signal and sampled it at $F_s = 12$ kHz.

The probability density function (PDF) for the voice coil position is drastically different for simple sine stimuli compared to regular program content such as music and speech. The PDF for a sine signal has a bathtub shape. A voice coil excited with a sine signal spends the majority of the time at extremal positions, because it has the lowest velocity at those points. A voice coil excited with music or speech spends the majority of the time around the rest position [14]. Its PDF has a Gaussian bell shape. Figure 9 shows the empirical PDFs of the voice coil position for the applied sine and pseudo-music signals in the improved driver. From Figure 9, it becomes evident that sine signals are suboptimal to determine relevant nonlinear effects in regular program material.

The fact that the voice coil spends the majority of the time around the rest position when regular content is played could lead to the notion that the flux modulation for regular content is less severe than it is for pure sine signals. However, flux modulation is a function of voice coil velocity and gradient of inductance (see last term in Equation (1)). Plotting the $Bl(x(t))$ phase clearly shows that flux modulation for pseudomusic content is more detrimental than it is for pure sine signals. Figure 10 shows the phase plots for the two driver motor configurations.

Comparing with the simple sine results in Figure 6, it becomes evident that flux modulation is more relevant for complex music signals. Comparison of Figures 10 a) and c) shows that the added shorting rings and the slight change in pole structure had a dramatic effect on the flux modulation. Not only did it decrease the spread of the $Bl(x(t))$ lines, it also made them much smoother. This effect is also visible in Figures 10 b) and d). Flux modulation is not something that can be studied directly with a LP model, because the effect is inherently tied to the driver geometry and material configuration.

For sake of completeness we also report the rRMSE values between simulation and measurement for position, acceleration and current for the improved driver geometry. The FE prediction for voice coil position had an rRMSE value of 3.85 % compared to the measurement. The prediction for acceleration had an rRMSE value of 24 % and the current had an rRMSE value of 21 %.

## 4 Discussion

The results in previous section demonstrate the current capabilities of the presented fully coupled time-domain simulation method. While the results for the voice coil position show an rRMSE error of less than 5 % compared to a measurement and an LP model, the results for acceleration and voice coil current were less accurate. Nonetheless, we demonstrated that the presented method can reveal previously unavailable insight into the flux modulation. This finding provides transducer

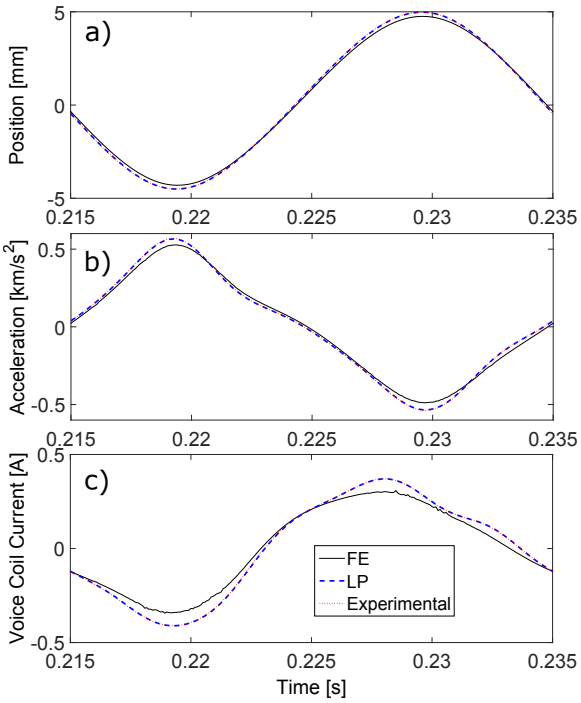


**Fig. 7:** Simulated and measured Position (a), acceleration (b), and current (c) for a sine wave applied to the improved motor design at steady state. The FE model result tracks the measured distorted position and acceleration signal. Compared to the measurement the The FE model has rRMSE of 4.63 % for the position, 7.60 % for the acceleration, and 15.9 % for the current. The LP model is indistinguishable from the measurement.

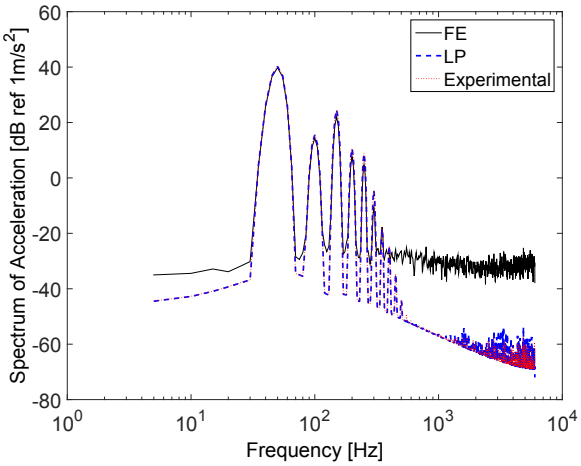


**Fig. 8:** Simulated and measured acceleration spectrum for a sine wave applied to the improved motor design. The harmonic content is clearly represented in the FE model data.

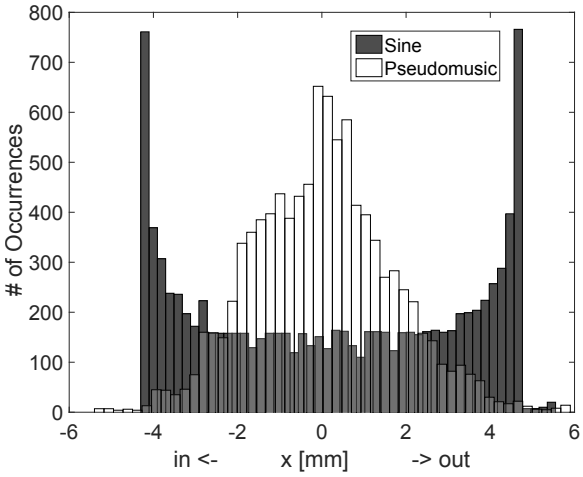


**Fig. 9:** The PDFs of the voice coil position for the improved motor geometry. The dark histogram is calculated for a 1 s long 50 Hz sine tone. The white histogram is calculated from a 1s long pseudomusic signal. Both signals were sampled at 12 kHz.

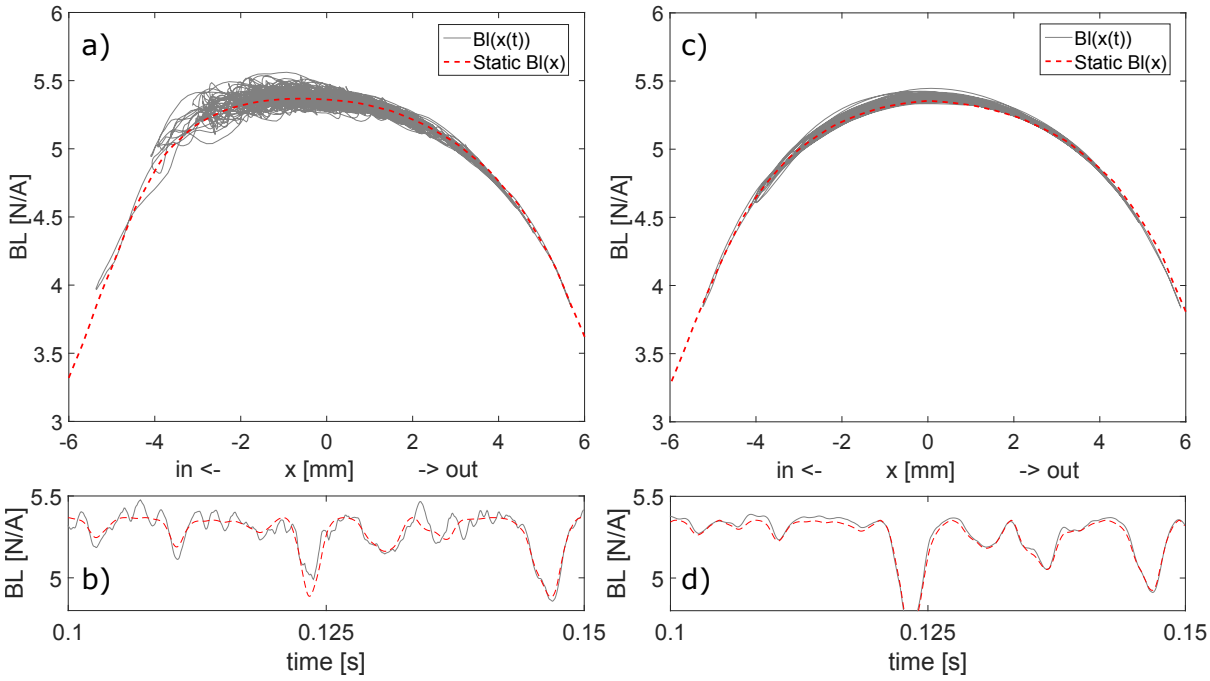


**Fig. 10:** Static (dashed red) and modulated (solid grey) $Bl$ plots for the simple (left) and improved (right) motor configurations. Plots a) and c) show the $Bl(x(t))$ phase plot and plots b) and d) show the $Bl$ values over a short time period.

engineers with additional information and detailed insight into the nonlinear behavior of their designs. With a fully-coupled, time-dependent FE simulation, it is now possible to study and predict motor behavior for signals more akin to speech and music. This is not directly possible with frequency domain simulations that are only valid for small displacements around the linearization point.

We have also shown some limitations of the presented method and we offer some potential explanations for the mismatch between simulation and measurements. A better characterization of the magnet used in the physical sample will likely reduce the error between predicted and measured $Bl(x)$ curve. Possibly it is also necessary to include the metal frame to account for a more accurate fringe field.

The FE model tracks the position of the voice coil compared to the measurement within 5 % accuracy. For the acceleration, which is directly linked to sound pressure in the frequencies below diaphragm breakup, we are seeing larger errors. One possible explanation for the very large 24 % rRMSE between FE model and measured acceleration in the case of pseudomusic stimulus could be that the physical sample was driven with an input signal of 48 kHz. The FE model used a down-sampled 12 kHz version of the same signal, missing out on higher frequency content and reducing local extrema.

The time-domain results for acceleration and current may suggest that the FE model is not a good predictor for the distortion caused by a given loudspeaker motor design, but the frequency domain analysis discredits that statement to some extent. The FE model spectrum clearly shows the harmonic distortion peaks for the pure sine input signal. The relatively higher noise-floor level for the FE model is broadband, akin to white noise, and is therefore likely caused by numerical errors, and can be corrected by a tighter tolerance on the solver.

Direct comparison with a measurement is a tough challenge for any loudspeaker design modeler. While the presented method is not yet ripe for a full characterization of the acceleration response, it does offer some improvement over existing simulation methods. In particular, it is now possible to study the effects of flux

modulation even before a physical sample or prototype is built.

## 5 Summary

We have presented a novel approach to the prediction of loudspeaker motor performance via direct FE simulations in the time domain. The suggested FE modeling method only requires a motor geometry and materials parameters to obtain time-dependent position and acceleration signals of the voice coil. The model consists of a fully coupled system of FE electromagnetic model and an ODE for the excursion of the voice coil.

We have simulated two separate driver geometries and applied two input signals to each. The results have been compared with an LP model and an measurement of a physical sample. The FE model time-domain results for the position are within 5 % error, but the results for acceleration and current are larger. However, the model provides previously unavailable insight into the flux modulation. As such, the presented method can be used to optimize driver motor configurations and mitigate detrimental effects of flux modulation.

The presented method can be used to compare different motor geometries before the prototyping stage, which is a useful tool for loudspeaker transducer engineers. Future work will be conducted to improve the accuracy and reliability of the predictions when compared to measurements on physical samples.

## 6 Acknowledgments

Samsung Electronics and Samsung Research America supported this work. The authors would like to thank the staff of Samsung's US Audio Lab who helped with the manufacturing and measurement of the physical sample, offered helpful suggestions, rewieved the manuscript, and contributed to its content.

## References

[1] Svobodnik, A., Shively, R., and Chauveau, M., "Multiphysical Simulation Methods for Loudspeakers - Advanced CAE-Based Simulations of Motor Systems," in *Audio Eng. Soc. Conv.*, 137, 2014, no.9214.

[2] Kaltenbacher, M., *Numerical Simulation of Mechantronic Sensors and Actuators*, Springer, 2015.

[3] COMSOL, "COMSOL Multiphysics User Guide," 2016, http://www.comsol.com.

[4] Voishvillo, A. and Kochendörfer, F., "Application of Static and Dynamic Magnetic Finite Element Analysis to the Design and Optimization of Moving Coil Transducer Motors," in *Audio Eng. Soc. Conv.*, 135, 2013, no.8989.

[5] Dodd, M., Klippel, W., and Oclee-Brown-J., "Voice Coil Impedance as a Function of Frequency and Displacement," in *Audio Eng. Soc. Conv.*, 117, 2004, no.6178.

[6] Kochendörfer, F. and Voishvillo, A., "Nonlinear Flux Modulation Effects in Moving Coil Transducers," in *Audio Eng. Soc. Conv.*, 137, 2014, no.9162.

[7] Dodd, M., "The Transient Magnetic Behaviour of Loudspeaker Motors," in *Audio Eng. Soc. Conv.*, 111, 2001, no.5410.

[8] Klippel, W., "Tutorial: Loudspeaker Nonlinearities - Causes, Parameters, Symptoms," *J. Audio Eng. Soc.*, (54), pp. 907–939, 2006.

[9] Klippel, W., "Measurement of large-signal parameters of electrodynamic transducer," in *Audio Eng. Soc. Conv.*, 107, 1999, no.5008.

[10] Vanderkooy, J., "A Model of Loudspeaker Driver Impedance Incorporating Eddy Currents in the Pole Structure," *J. Audio Eng. Soc.*, (37), pp. 119–128, 1989.

[11] Button, D. J., "Design Parameters and Trade-Offs in Large Diameter Transducers," in *Audio Eng. Soc. Conv.*, 91, 1991, n0.3192.

[12] Halvorsen, M., Tinggard, C., and Agerkvist, F. T., "Flux Modulation in the Electrodynamic Loudspeaker," in *Audio Eng. Soc. Conv.*, 138, 2105, no.9317.

[13] Ascher, U. and Petzold, L., *Computer Methods for Ordinary Differential Equations and Differential-Algebraic Equations*, SIAM, 1998.

[14] Chapman, P. J., "Programme Material Analysis," in *Audio Eng. Soc. Conv.*, 100, 1996, no.4277.